Through-Bond and Chain-to-Chain Coupling. Two Pathways in Electron Tunneling through Liquid Alkanethiol Monolayers on Mercury Electrodes

Krzysztof Slowinski,[†,‡] Richard V. Chamberlain,[†] Cary J. Miller,*[,§] and Marcin Majda*[,†]

Contribution from the Department of Chemistry, University of California at Berkeley, Berkeley, California 94720-1460, Department of Chemistry and Biochemistry, University of Maryland, College Park, Maryland 20742, and Department of Chemistry, Warsaw University, Pasteura 1, 02-093 Warsaw, Poland

Received June 11, 1997. Revised Manuscript Received September 18, 1997[⊗]

Abstract: Formation, structure, and properties of alkanethiolate monolayers on micrometrically driven hanging mercury drop electrodes were investigated electrochemically. Alkanethiols with the chain length from C_8 to C_{18} were shown to form densely packed (ca. 20.3 Å^2/molecule for $C_{12}SH$), perpendicularly oriented monolayers on mercury in a process involving two electron oxidation of Hg to form mercuric thiolate, in agreement with earlier literature reports for a number of thiols. Electron tunneling rates across these films (due to $Ru(NH_3)_6^{3+}$ electro-reduction in aqueous 0.50 M KCl) exhibit characteristic exponential increase with the electrode potential (with transfer coefficient $\alpha = 0.25$), and an exponential decay with the monolayer thickness (with a through-bond decay constant, $\beta_{tb} = 1.14$ per methylene group or 0.91 Å^{-1}). Slow stepwise expansion of the mercury drop electrodes coated with alkanethiolates (C_9-C_{14} only) results in an only small increase of the tunneling current maintaining the pin-hole free structure of the monolayers. Capacitance measurements showed that the film thickness changes inversely proportionally with the electrode surface area. The increase of the tunneling current recorded in the drop expansion experiments was accounted for by postulating existence of an additional tunneling pathway involving chain-to-chain coupling. Data analysis in view of this parallel pathways model yielded a through-space decay constant, $\beta_{ts} = 1.31$ Å^{-1}. *Ab initio* computations of the electronic coupling matrix element (based on Koopmans' theorem approximation) and its distance dependence across a number of perpendicularly orientated n-alkanes yielded a decay constant of 1.25 Å^{-1} in excellent agreement with the measurements.

Introduction

How the intervening medium between a donor and acceptor controls the rate of electron transfer remains a largely unsolved problem of crucial scientific importance. Long-range electron transfer reactions play pivotal roles in a host of biological systems[1−3] and are crucial to the design of electronic devices composed of molecular units.[4] In recent years, increasing attention, both experimental and theoretical, has been focussed on delineating the structural dependence of long-range electron transfers. For strongly nonadiabatic electron transfers, the electron transfer rate depends on the strength of the electronic coupling between the donor and acceptor mediated by the structure of the intervening space.[5] In the Fermi's golden rule limit appropriate for weakly electronically coupled systems, the electron transfer rate is proportional to the square of the electronic coupling matrix element, H_{ab}^2. Investigations of the role of the intervening medium in electron transfer, therefore, reduce to a question of the strength of electronic coupling through specific types of molecular media.[6]

Early experimental work on electron tunneling relied on Langmuir−Blodgett monolayer and multilayer assemblies[7] and involved electrical conductivity[8,9] and photoinduced electron transfer measurements.[10] Many recent advances in the studies of the intervening medium effects in electron tunneling have been made using the following two experimental approaches. In the first, synthetic donor/acceptor pairs are separated by rigid molecular spacer groups of controlled length and structure.[11−18] In the second, investigations involve redox proteins in which

[†] University of California at Berkeley.
[‡] Warsaw University.
[§] University of Maryland.
[⊗] Abstract published in *Advance ACS Abstracts,* November 1, 1997.

(1) *Structure and Bonding: Long Range Electron Transfer in Biology*; Springer-Verlag: New York, 1991.
(2) *Metal Ions in Biological Systems: Electron Transfer Reactions in Metalloproteins*; Marcel Dekker: New York, 1991; Vol. 27.
(3) Gray, H. B.; Winkler, J. R. *Annu. Rev. Biochem.* **1996**, *65*, 537−561.
(4) *Molecular Electronics - Science and Technology: AIP Conference Proceedings*; Aviram, A., Ed.; American Institute of Physics: 1992; Vol. 262.
(5) Marcus, R. A.; Sutin, N. *Biochim. Biophys. Acta* **1985**, *811*, 265−322.
(6) Newton, M. D. *Chem. Rev.* **1991**, *91*, 767−792.
(7) Kuhn, H.; Moebius, D. in *Investigations of Surfaces and Interfaces-Part B*; *Physical Methods of Chemistry Series*, 2nd ed.; Rossiter, B. W., Baetzold, R. C., Eds.; John Wiley & Sons, Inc.: 1993; Vol. IXB, Chapter 6, pp 375−542.
(8) Mann, B.; Kuhn, H. *J. Appl. Phys.* **1971**, *42*, 4398.
(9) Polymeropoulos, E. E.; Sagiv, J. *J. Chem. Phys.* **1978**, *69*, 1836.
(10) Moebius, D. *Acc. Chem. Res.* **1981**, *14*, 63−68.
(11) Closs, G. L.; Miller, J. R. *Science* **1988**, *240*, 440.
(12) Liang, N.; Miller, J. R.; Closs, G. L. *J. Am. Chem. Soc.* **1990**, *112*, 5353−5354.
(13) Vassilian, A.; Wishart, J. F.; Hemelryck, B. V.; Schwarz, H.; Issied, S. S. *J. Am. Chem. Soc.* **1990**, *112*, 7278−7296.
(14) Ogawa, M. J.; Wishart, J. F.; Young, Z.; Miller, J. R.; Isied, S. S. *J. Phys. Chem.* **1993**, *97*, 11456−11463.
(15) Paulson, B.; Eaton, P.; Closs, G. L.; Miller, J. R. *J. Phys. Chem.* **1993**, *97*, 13042−13045.
(16) Meade, T. J.; Kayem, J. F. *Angew. Chem., Int. Ed. Engl.* **1995**, *34*, 352−354.
(17) Larson, S. L.; Hendrickson, S. M.; Ferrere, S.; Derr, D. L.; Elliott, C. M. *J. Am. Chem. Soc.* **1995**, *117*, 5881−5882.
(18) Paulson, B. P.; Curtiss, L. A.; Bal, B.; Closs, J. L.; Miller, J. R. *J. Am. Chem. Soc.* **1996**, *118*, 398.

S0002-7863(97)01921-5 CCC: $14.00

an electron acceptor (or donor) is attached to a specific site on the periphery of a protein.[3,19−21] This approach has yielded some of the most intricate and insightful information to date concerning the dependence of the tunneling rates on the chemical structure of specific pathways within the polypeptide matrix separating donor and acceptor sites.

A theoretical model proposed by Beratan and Onuchic and their co-workers to describe the structural dependence of long-range electron transfers in biological systems relies on the identification of electronic coupling pathways along the molecular framework.[22−26] This approximation reduces the many body electronic coupling problem to a more tractable sum of paths containing covalent, hydrogen bonds and van der Waals bridges (through space jumps). Each of these steps is assigned a coupling constant, and the efficiency of the entire pathway is then computed as a product of the series of the individual units. By analyzing a large number of pathways, the model can identify those that are most efficient. This approach allowed Gray and co-workers to compare, for example, tunneling efficiencies through pathways encompassing β-sheets and α-helices.[27,28]

The application of this pathway approach depends critically on determining the electronic coupling through each of the elementary coupling steps. Given the structural complexity of the protein systems, the isolation and study of these individual coupling steps using modified proteins is a difficult proposition. A simpler approach in which one relies on electrochemical measurements of electron tunneling rates across molecular films immobilized at the electrode surface has also been successfully explored[29,30] and begins to constitute the third general approach in the investigations of electron tunneling kinetics. Most commonly, alkanethiol derivatives are chemisorbed on gold electrodes forming compact crystalline monolayers.[31,32] The electron transfer from the electrode to redox probes, either covalently attached to the monolayer periphery[33] or freely diffusing in the electrolyte solution,[34] proceeds via a long-range electron tunneling. Such electron transfer measurements can yield a wealth of information concerning the structural dependence of the long-range electron coupling through molecular media. Assuming that the major pathway across monolayers in which the chains are tilted ca. 30° involves tunneling through σ-bonds, the decay constants in the range 0.78−0.97 $Å^{-1}$ were reported.[31,34−39] These values are in good agreement with the theoretical predictions.[40−42] Recently, the influence of atomic level modifications in the structure of the alkane chains[43] and quantum interference effects[44] have also been probed. Replacement of one methylene unit by ether, olefin, or alkyne fragments decreased the electronic coupling across the monolayer, a result consistent with *ab initio* calculations.

The strength of these electrochemical measurements has been in probing the electronic coupling through covalently linked atoms. The efficiency of electron transfers between nonbonded atoms is harder to study, especially at the solid electrodes. We reported recently preliminary results of electron tunneling measurements in which alkanethiol monolayers were self-assembled on hanging mercury drop electrodes (HMDE).[45] To summarize briefly, we discovered that alkanethiols with chain length varying between C_9 and C_{14} form liquid monolayers that maintain their defect-free, impermeable characteristics even when the surface area (A) of a HMDE is increased by as much as 30%. We showed that a gradual expansion of a mercury drop carrying an alkanethiol monolayer results in a concurrent decrease of the monolayer thickness (d) such that the volume of the film stays constant (Ad = const). This allowed us to follow the dependence of the electron tunneling current (in electroreduction of $Ru(NH_3)_6^{3+}$) on the film thickness. The increase of current that we observed upon HMDE expansion was more than an order of magnitude smaller than expected if an alkanethiol monolayer is assumed to be an isotropic dielectric barrier. Clearly, electron tunneling across alkanethiol monolayers proceeds predominantly along a pathway involving σ-bonded alkyl chains. Since the length and thus the tunneling efficiency along that pathway should remain largely invariant with monolayer expansion, we postulated that the small current increase observed during the drop expansion reveals the contribution of a second, much less efficient pathway, involving chain-to-chain coupling. In this report, we present a more thorough investigation of this system and focus on the quantitative assessment of the electron tunneling efficiency along the two pathways.

Experimental Section

Reagents. Fresh samples of the alkanethiols, $H(CH_2)_nSH$, n = 10, 12, 14, 16, 18, were purchased from TCI America (95+%); nonanethiol (95%) was purchased from Aldrich. They were used as received. α,ω-Hydroxyalkanethiols, $HO(CH_2)_nSH$, n = 10, 11, 12, 14, were synthesized as described previously.[34] Mercury (Quicksilver Products Inc., triply distilled) was used without further purification. The following reagents were also used as received: hexaammineruthenium(III)chloride (Strem, 99%), hexadecane (Aldrich, 99+% anhydrous), chloroform (Aldrich, reagent grade), ethanol (Fisher, reagent grade), methanol

(19) Winkler, J. R.; Gray, H. B. *Chem. Rev.* **1992**, *92*, 369−379.
(20) Moser, C. C.; Keske, J. M.; Warncke, K.; Farid, R. S.; Dutton, P. L. *Nature* **1992**, *355*, 796−802.
(21) Bjerrum, M. J.; Casimiro, D. R.; I-J., C.; Di Billo, A. J.; Gray, H. B.; Hill, M. G.; Langen, R.; Mines, G. A.; Skov, L. K.; Winkler, J. R.; Wuttke, D. S. *J. Bioenerg. Biomembr.* **1995**, *27*, 295.
(22) Onuchic, J. N.; Andrade, P. C. P.; Beratan, D. N. *J. Chem. Phys.* **1991**, *95*, 1131.
(23) Beratan, D. N.; Betts, J. N.; Onuchic, J. N. *Science* **1991**, *252*, 1285−1288.
(24) Onuchic, J. N.; Beratan, D. N.; Winkler, J. R.; Gray, H. B. *Annu. Rev. Biophys. Biomol. Struct.* **1992**, *21*, 349−377.
(25) Beratan, D. N.; Onuchic, J. N.; Winkler, J. R.; Gray, H. B. *Science* **1992**, *258*, 1740−1741.
(26) Curry, W. B.; Grabe, M. D.; Kurnikov, I. V.; Skourtis, S. S.; Beratan, D. N.; Regan, J. J.; Aquino, A. J. A.; Beroza, P.; Onuchic, J. N. *J. Bioenerg. Biomembr.* **1995**, *27*, 285−293.
(27) Langen, R.; Chang, I.-J.; Germanas, J. P.; Richards, J. H.; Winkler, J. R.; Gray, H. B. *Science* **1995**, *268*, 1733−1735.
(28) Langen, R.; Colon, J. L.; Casimiro, D. R.; Karpishin, T. B.; Winkler, J. R.; Gray, H. B. *J. Biol. Inorg. Chem.* **1996**, *1*, 221−225.
(29) Li, T. T.-T.; Weaver, M. J. *J. Am. Chem. Soc.* **1984**, *106*, 6107−6108.
(30) Forster, J. R.; Faulkner, L. R. *J. Am. Chem. Soc.* **1994**, *116*, 5444−5452.
(31) Dubois, L. H.; Nuzzo, R. G. *Annu. Rev. Phys. Chem.* **1992**, *43*, 437.
(32) Finklea, H. O. *Electrochemistry of Organized Monolayers of Thiols and Related Molecules on Electrodes* in *Electroanalytical Chemistry*; Bard, A. J., Rubinstein, I., Eds.; Marcel Dekker: New York, 1996; Vol. 19, pp 109−335.
(33) Chidsey, C. E. D. *Science* **1991**, *251*, 919−922.
(34) Becka, A. M.; Miller, C. J. *J. Phys. Chem.* **1992**, *96*, 2657−2668.
(35) Xu, J.; Li, H.-L.; Zhang, Y. *J. Phys. Chem.* **1993**, *97*, 11497−11500.
(36) Smalley, J. F.; Feldberg, S. W.; Chidsey, C. E. D.; Linford, M. R.; Newton, M. D.; Liu, Y.-P. *J. Phys. Chem.* **1995**, *99*, 13141−13149.
(37) Carter, M. T.; Rowe, G. K.; Richardson, J. N.; Tender, L. M.; Terrill, R. H.; Murray, R. W. *J. Am. Chem. Soc.* **1995**, *117*, 2896−2899.
(38) Finklea, H. O.; Hanshew, D. D. *J. Am. Chem. Soc.* **1992**, *114*, 3173−3181.
(39) Finklea, H. O.; Liu, L.; Ravenscroft, M. S.; Punturi, S. *J. Phys. Chem.* **1996**, *100*, 18852−18858.
(40) Curtiss, L. A.; Naleway, C. A.; Miller, J. R. *J. Phys. Chem.* **1993**, *97*, 4050−4058.
(41) Liang, C.; Newton, M. D. *J. Phys. Chem.* **1993**, *97*, 3199−3211.
(42) Hsu, C.-P.; Marcus, R. A. *J. Chem. Phys.* **1997**, *106*, 584−598.
(43) Cheng, J.; Saghi-Szabo, G.; Tossell, J. A.; Miller, C. J. *J. Am. Chem. Soc.* **1996**, *118*, 680−684.
(44) Cheng, J.; Miller, C. J. *J. Phys. Chem.* **1997**, *101*, 1058−1062.
(45) Slowinski, K.; Chamberlain, R. V.; Bilewicz, R.; Majda, M. *J. Am. Chem. Soc.* **1996**, *118*, 4709−4710.

(Fisher, spectroscopic grade), KCl (Fisher, ACS grade), $NaClO_4$ (Fisher, purified grade). Octadecyltrichlorosilane, OTS (Petrarch Systems), was vacuum distilled and sealed in small glass ampules that were opened immediately prior to the individual experiments. House-distilled water was passed through a four-cartridge Barnstead Nanopure II purification system. Its resistivity was in the range 17.6−18.3 MΩ cm.

Synthesis of Mercuric Dodecanethiolate. Dodecanethiol (1.14 g) was dissolved in 25 mL of chloroform and combined with a large excess of mercury. Formation of a gray precipitate was immediately apparent on the Hg surface. The mixture was stirred for 4 days at room temperature to assure completeness of the reaction. Subsequently, the chloroform suspension of the precipitate was decanted. Chloroform (50 mL) was used to wash the unreacted mercury and to dissolve the remaining precipitate. The chloroform solutions were combined, heated gently to dissolve the precipitate, filtered, and cooled in an ice bath. The resulting white-gray precipitate was separated by vacuum filtration and dried in a vacuum oven at room temperature for 48 h. The elemental analysis results: C 47.52%, H 8.34%, S 10.44%, Hg 33.70% (by difference) agreed with the calculated values for $[CH_3(CH_2)_{11}S]_2$-Hg: C 47.78%, H 8.35%, S 10.63%, Hg 33.24%.

Hanging Mercury Drop Electrode. A Kemula-Kublik type HMDE[46] was constructed using a slightly modified design described recently by Guidelli and co-workers.[47] A 1.50 mm diameter precision stainless steel rod was driven by a micrometric screw (Digimatic Micrometer Head by Mitutoyo, Model 350-712-10 with ±1 μm resolution) to create a Hg drop of desired size at the tip of a glass capillary. In the Hg drop expansion experiments 400 μm diameter capillaries were used. In coulometric experiments 250 μm capillaries were used. They were periodically cleaned with hot nitric acid, rinsed with water and ethanol, dried, and silanized with OTS. Precision of the correlation between micrometric drop extrusion and its surface area was ±0.1% obtained via weight measurement assuming drop sphericity less the cross-sectional area of the orifice of the capillary. The precision of dialing a single Hg drop electrode of a specific surface area was determined voltammetrically to be ±0.5% (largely due to uncertainty in setting the initial position of Hg in the capillary). Agreement of the differential capacitance measured with the bare Hg drop electrodes in aqueous KCl electrolytes with the literature data[48] was used as a criterion of cleanliness of the mercury/solution interface.

Self-assembly of alkanethiol monolayers was carried out from 10−20% hexadecane solutions, while α,ω-hydroxyalkanethiol monolayers were assembled from saturated ethanol solutions. The incubation time was typically 5 min. Due to the very rapid kinetics of the Hg alkanethiol reaction (see Results and Discussion section), longer incubation times, up to several hours, did not change the properties of the resulting monolayer films. Following the self-assembly, the HMDE was rinsed with ethanol for 10 s and with water for 5 s before the electrochemical cell was raised up to submerge the electrode in the electrolyte solution. During all these steps, the electrode was clamped in a fixed position to avoid accidental dislodging of the hanging drop.

Contact Angle Measurements. Advancing contact angles of water on mercury coated with monolayers of alkanethiols were carried out on a fresh mercury pool confined in an OTS-silanized glass cylinder (2 cm in diameter) which was fixed vertically in a crystallization dish. A second glass cylinder, slightly longer and of slightly larger diameter, was placed concentrically around the first one. Mercury formed a flat meniscus extending above the edge of the inner cylinder. A hexadecane or an ethanol self-assembly solution was poured over the mercury and allowed to make contact with it for at least 1 min. By lifting the outer glass cylinder, the self-assembly solution was allowed to drain into the crystallization dish. The same method was then used to rinse the surface of mercury repeatedly with ethanol and water without disturbing it. The contact angles were measured with a Ramé-Hart Model 100 contact angle goniometer. The entire apparatus was placed on a vibration-isolation table.

Electrochemical Measurements. All electrochemical measurements were done with a BAS 100A electrochemical analyzer using a two compartment cell at room temperature of ca. 20 °C. The voltammetric tunneling currents were corrected for capacitive current by digital background subtraction. All potentials were measured and are reported vs saturated calomel reference electrode (SCE).

***Ab Initio* Calculations.** *Ab initio* computations were performed using GAMESS[49] running on a Model 250 Alpha Station. Making use of the Koopmans' theorem approximation for the electronic coupling matrix element, we calculate the splitting energies of neutral Li−Li triplet using an unrestricted Hartree−Fock SCF calculation.[43] The geometries of all the hydrocarbon spacers used were optimized at the 3-21G basis set level prior to the introduction of the Li reporter atoms.[50−52] The lithium radical reporter atoms were positioned symmetrically on both sides of the hydrocarbon chains at 4 Å from the central methylene group (for the β_{ts} calculations) or from the terminal methyl groups of the hydrocarbon chains (for the β_{tb} calculations).

Results and Discussion

The experimental results presented below fall into two categories. First, we report results describing formation, structure, and properties of alkanethiol monolayers on mercury. Of crucial importance in this part is the determination of the perpendicular orientation of the alkanethiolate chains with respect to the Hg surface and characterization of the physical properties of these films during Hg drop expansion experiments. Electron tunneling experiments involving both native and expanded films constitute the second category of the experimental results. Presentation of the parallel pathways model of electron tunneling involving through-bond and through-space (chain-to-chain coupling) pathways and extraction of their respective decay constants are the key elements of that group of results.

Formation of Alkanethiol Monolayers on Hg. Early investigations of the electrode reactions of thio-compounds such as cysteine on mercury under potentiostatic conditions postulated oxidation of mercury with concurrent formation of mercuric or mercurous thiolate,[53,54] according to the following

$$n\mathrm{RSH} + \mathrm{Hg} - ne^- \rightarrow \mathrm{Hg(SR)}_n + n\mathrm{H}^+ \quad n = 1 \text{ or } 2$$

More recent electrochemical studies of alkanethiols in aqueous basic solutions[55] and in nonaqueous media[56] showed formation of mercuric thiolates. Structure and passivating properties of alkanethiols on Hg have also been investigated.[57−60] Thus, regardless of the oxidation state of mercury, alkanethiol self-assembly is associated with a transfer of one electron per thiol. This is in contrast with only partial electron transfer (ca. 0.3 electron per thiol) in oxidative coupling of alkanethiols to

(46) Kemula, W.; Kublik, Z. *Anal. Chim. Acta* **1958**, *18*, 104.
(47) Becucci, L.; Moncelli, M. R.; Guidelli, R. *J. Electroanal. Chem.* **1996**, *413*, 187−194.
(48) Grahame, D. C. *J. Am. Chem. Soc.* **1949**, *71*, 2975.
(49) Schmidt, M. W.; Baldridge, K. K.; Boatz, J. A.; Elbert, S. T.; Gordon, M. S.; Jensen, J. H.; Koseki, S.; Matsunaga, N.; Nguyen, K. A.; Su, S.; Windus, T. L.; Dupuis, M.; Montgomery, J. A., Jr. *J. Comput. Chem.* **1993**, *14*, 1347−1363.
(50) Binkley, J. S.; Pople, J. A.; Hahre, W. J. *J. Am. Chem. Soc.* **1980**, *102*, 939−947.
(51) Gordon, M. S.; Binkley, J. S.; Pople, J. A.; Pietro, W. J.; Hehre, W. J. *J. Am. Chem. Soc.* **1982**, *104*, 2797−2803.
(52) Pietro, W. J.; Francl, M. M.; Hehre, W. J.; DeFrees, D. J.; Pople, J. A. *J. Am. Chem. Soc.* **1982**, *104*, 5039−5048.
(53) Kolthoff, I. M.; Barnum, C. *J. Am. Chem. Soc.* **1940**, *62*, 3061−3065.
(54) Kolthoff, I. M.; Stricks, W.; Tanaka, N. *J. Am. Chem. Soc.* **1955**, *77*, 4739−4742.
(55) Birke, R. L.; Mazorra, M. *Anal. Chim. Acta* **1980**, *118*, 257−269.
(56) Peter, F.; Rosset, R. *Anal. Chim. Acta* **1975**, *79*, 47−58.
(57) Bruckner-Lea, C.; Janata, J.; Conroy, J.; Pungor, A.; Caldwell, K. *Langmuir* **1993**, *9*, 3612−3617.
(58) Demoz, A.; Harrison, D. J. *Langmuir* **1993**, *9*, 1046.
(59) Bruckner-Lea, C.; Kimmel, R. J.; Janata, J.; Conroy, J. F. T.; Caldwell, K. *Electrochim. Acta* **1995**.
(60) Muskal, N.; Turyan, J.; Mandler, D. *J. Electroanal. Chem.* **1996**, *409*, 131−136.

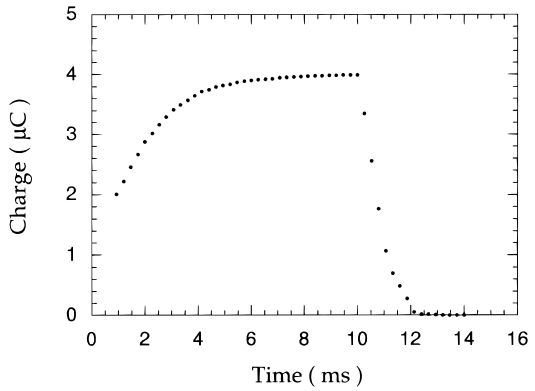

Figure 1. A double-potential step chronocoulometric transient recorded at a HMDE ($A = 0.0465$ cm^2) in a 0.02 M dodecanethiol, 0.50 M $NaClO_4$ methanol solution. The electrode potential was stepped from −1.0 to −0.3 V for 10 ms and then returned to the initial value.

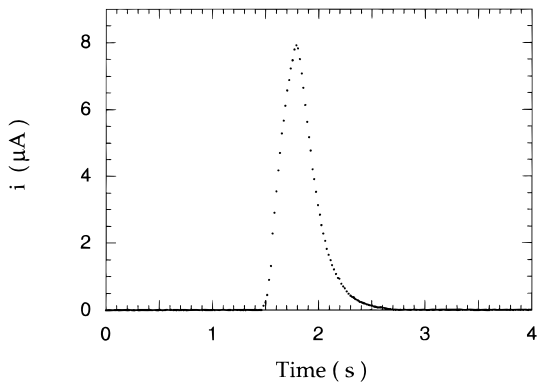

Figure 2. A constant potential ($E = 0.0$ V vs SCE) current-time transient recorded in response to a HMDE extrusion in a 0.02 M dodecanethiol, 0.50 M $NaClO_4$ methanol solution. The electrode surface area was initially limited to the cross-sectional area of the HMDE capillary (ca. 0.0005 cm^2) and then expanded at $t \approx 1.5$ s to 0.0447 cm^2.

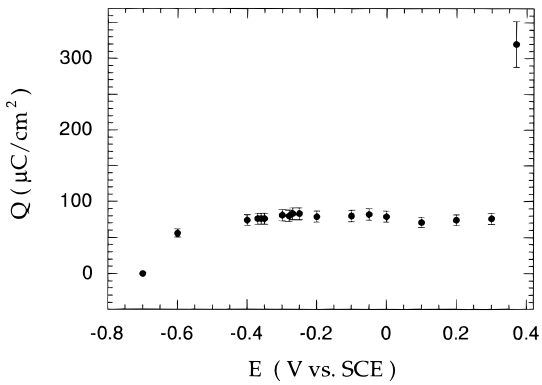

Figure 3. A plot of charge vs electrode potential due to mercuric dodecanethiolate formation obtained in the constant potential Hg drop extrusion experiments such as that in Figure 2. The data points represent averages (and standard deviations) of at least 10 experiments carried out at each value of the electrode potential.

gold.[61] As described in the Experimental Section, we carried out bulk synthesis of mercury dodecanethiolate. Following isolation and purification of the product, elemental analysis revealed 1:2 atomic ratio of Hg:S indicating that a two electron oxidation of mercury to mercuric dodecanethiolate takes place under the conditions of the chemical oxidation.

The known stoichiometry of the electrode reaction leading to alkanethiol self-assembly allowed us to measure the packing density of thiols on Hg. First, to assess the kinetics of self-assembly, we carried out standard chronocoulometric experiments using typically 0.02 M solution of a thiol in 0.50 M methanolic $NaClO_4$ solution. Initially, a HMDE was held at a sufficiently negative potential (−1.00 V vs SCE) to prevent self-assembly. A short potential pulse increasing the HMDE potential to −0.30 V was applied and charge vs time recorded. Results of a typical chronocoulometric experiment done with a dodecanethiol are shown in Figure 1. It is apparent that the anodic charge levels off after less than 8 ms, demonstrating that self-assembly of a full monolayer which blocks further oxidation of mercury is essentially instantaneous under these conditions. The value of the plateau charge in Figure 1, 8.6×10^{-5} C/cm^2, is a sum of the charge due to oxidative formation of mercuric thiolate monolayer and the double-layer charge. The latter is not negligible and is difficult to measure accurately. At the initial potential of −1.00 V, the mercury surface is negatively charged, and its capacitance is on the order of 20 μF/cm^2.[48] This negative double-layer charge has to be removed upon monolayer formation since the final capacitance of the coated electrode is only ca. 1.0 μF/cm^2 (see data below).

To circumvent the uncertainties related to double-layer charging, we resorted to constant potential coulometry experiments. In this approach, the HMDE is held at a potential at which formation of mercuric thiolate is allowed, and a fresh drop of precisely known surface area is rapidly extruded. This is easily accomplished with a micrometrically driven HMDE (see Experimental Section). Current is measured as a function of time during electrode extrusion and then integrated. A typical current-time transient recorded at 0.00 V vs SCE is shown in Figure 2 for a dodecanethiol. At $t = 0$, no current flows since the initially small electrode surface is covered by a passivating dodecanethiolate monolayer. A rapid current increase and its subsequent decay correspond to the formation of mercuric thiolate on a rapidly expanding Hg drop and its passivation. The integral of the current includes only a negligible double-layer charge component (<1 μC/cm^2 or ca. 1% of the total charge) since the interfacial capacitance of the newly created electrode is decreased substantially (to ca. 1 μF/cm^2) by the alkanethiol monolayer. The shape of the current time transients such as that in Figure 2 and the corresponding charge are independent of alkanethiol concentration, at least in the range 2×10^{-2}−2×10^{-5} M.

Using this approach, we investigated the dependence of the oxidative self-assembly charge and thus alkanethiol coverage on the electrode potential and the chain length. The charge vs potential data for dodecanethiol are shown in Figure 3. Stable, passivating monolayers can be formed in the range of −0.50 to +0.30 V vs SCE. Substantially larger or smaller coverages are obtained outside this range (see Figure 3). At potentials positive of 0.30 V, dodecanethiolate monolayers can no longer passivate the electrode against formation of multilayer quantities of mercuric thiolate. The average charge due to the monolayer formation (79 ± 8 μC/cm^2, an average and s.d. of at least 10 measurements at each of 15 different values of the electrode potential) corresponds to a surface concentration of 8.2×10^{-10} mol/cm^2 and to the mean molecular area of 20.3 Å^2/molecule. Coulometric coverage data for this and other alkanethiols are collected in Table 1. These experiments show, that regardless of the chain length, all alkanethiols form densely packed monolayers of perpendicularly or nearly perpendicularly oriented molecules.[62] This is in contrast with the characteristic ca. 30° tilt of the alkanethiols on gold.[31] Understandably, the gold-thiol epitaxy responsible for the tilt is not a factor in self-

(61) Krysinski, P.; Chamberlain, R. V.; Majda, M. *Langmuir* **1994**, *10*, 4286−4294.

Table 1. Characterization and Properties of Alkanethiolate Monolayers on Mercury

alkane-thiolate	Q^a [μC/cm^2]	mean molecular area^b [Å^2/molecule]	contact angle^c [deg]	capacitance [μF/cm^2]
C_8SH	77 ± 8 (30)	20.8		
C_9SH	70 ± 10 (30)	22.9	112 ± 4	1.30 ± 0.10 (10)
$C_{10}SH$	73 ± 9 (30)	21.9	112 ± 4	1.25 ± 0.08 (10)
$C_{12}SH$	79 ± 8 (150)	20.3	114 ± 4	1.04 ± 0.05 (30)
$C_{14}SH$	70 ± 12 (30)	22.9	114 ± 4	0.90 ± 0.09 (8)
$C_{16}SH$			116 ± 4	0.80 ± 0.10 (10)
$C_{18}SH$	80 ± 10 (30)	20.0	120 ± 8	0.74 ± 0.06 (10)
$HOC_{12}SH$			20 ± 10	

[a] Anodic charge due to oxidative formation of mercuric alkanethiolates; the numbers in parentheses correspond to the number of independent measurements used to report the average and standard deviations. [b] Average mean molecular area of alkanethiolates calculated from the charge values. [c] Advancing contact angle of water measured on alkanethiolate monolayer coated mercury surfaces (see Experimental Section).

assembly on the liquid mercury surface. Above ca. 0.30 V, much larger quantities of mercuric thiolate are formed because a single monolayer is no longer capable of passivating the electrode under the conditions of increasing driving force. Formation of mercuric dodecanethiolate is not possible at potentials below −0.65 V. Table 1 contains also results of the contact angle measurements carried out on mercury pool surfaces following self-assembly of the alkanethiols (see Experimental Section). These data, although burdened with a larger experimental error than those involving gold substrates, are consistent with the contact angles obtained for alkanethiol monolayers on gold.[31,63,64]

Properties of Mercuric Alkanethiolate Monolayers as Tunneling Barriers. A. Native Films. Additional information about the structure and properties of the alkanethiolate monolayers on mercury can be deduced from the capacitance measurements. These were done by fast scan (1 V/s) voltammetry in 0.5 M KCl. Characteristically rectangular i-E traces were recorded in the potential range −0.1 to −0.6 V. These gave the capacitance values listed for a number of alkanethiols in Table 1. Differential capacitance of these interfaces can be approximated by the Helmholtz model. The plot of 1/*C* vs film thickness for a number of alkanethiols is shown in Figure 4. Its slope yields a dielectric constant of 2.0, in good agreement with the literature data.[31,65,66] This confirms the perpendicular orientation of the alkyl chains. As reported previously, capacitances of the hydroxyalkanethiolate monolayers are slightly larger than those of the alkanethiolates with the same number of carbon atoms in the chain.[66,67]

Barrier properties of the alkanethiolate monolayers are best tested in the electron tunneling experiments. Figure 5 shows three cyclic voltammograms recorded with HMDE electrodes coated with nonane-, decane-, and dodecanethiolate monolayers. A 0.50 M KCl electrolyte containing 1.0 mM $Ru(NH_3)_6^{3+}$ was used. This ruthenium complex is known to be kinetically very fast (k_s > 0.2 cm s^{-1}).[68−70] In spite of this, the current-voltage

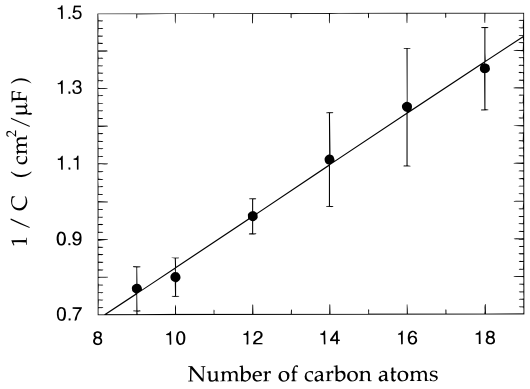

Figure 4. A plot of the reciprocal capacitance of the HMDE interface coated with alkanethiolate monolayers of different chain length (expressed in terms of the number of carbon atoms). The differential capacitance was measured by cyclic voltammetry (v = 1.0 V/s) in 0.50 M KCl electrolyte in the range −0.1 to −0.6 V vs SCE. The data points represent average values and standard deviations of 30 independent measurements for dodecanthiol and 10 for each of the other alkanethiols.

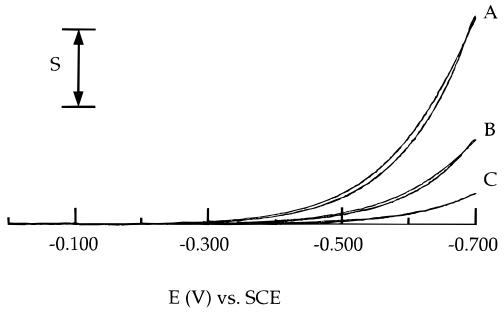

Figure 5. Cyclic voltammogram recorded in 1.0 × 10^{-3} M $Ru(NH_3)_6^{3+}$, 0.50 M KCl solution at the HMDE (A = 0.0230) coated with **A**, nonanethiolate; **B**, decanethiolate; **C**, dodecanethiolate monolayers; v = 50 mV/s. The scale bar coresponds to **A**, **B**, 500 nA; **C**, 100 nA.

curves exhibit low, scan rate independent, exponentially increasing current at potentials far negative of the formal potential of the ruthenium probe ($E^{\circ\prime}$ = −0.18 vs SCE). The hydroxy-terminated monolayers exhibit the same behavior. Clearly, in all cases, reduction of $Ru(NH_3)_6^{3+}$ is restricted to electron tunneling across the alkanethiolate films. (Under the conditions of Figure 5, the value of the diffusion controlled voltammetric peak current at a clean HMDE is 3.7 μA.) These results, together with the coulometric determination of the packing density and the capacitance data, concur with the notion that the alkanethiols form densely packed, pinhole-free monolayers on mercury. To assess the distance dependence of the electron tunneling, we plotted the natural logarithm of the current density (measured at −0.65 V)[71] vs film thickness (see Figure 6). The slope gave a decay constant β = 1.14 ± 0.09 per methylene group or 0.91 ± 0.08 Å^{-1} for both the methyl- and hydroxy-terminated monolayers. These values fall in the range of the literature data obtained with alkanethiol monolayers on gold electrodes.[31,34−39] It is interesting to note that the values of the tunneling current recorded under identical conditions are always larger for the hydroxy-derivatives of alkanethiols with the same number of chain carbon atoms. This difference corresponds to a ca. 1.2 Å difference in the tunneling distance (assuming again the perpendicular orientation of the alkyl chains). This is in spite of the fact that the hydroxy group adds approximately 1.1

(62) The area per molecule taken by the perpendicularly oriented, hexagonally closed-packed alkyl chains modeled as cylinders 4.75 Å in diameter is 19.5 Å^2. In contrast, the 30° tilt of alkanethiols on Au (111) increases the area per molecule to 22.6 Å^2.

(63) Bain, C. D.; Troughton, E. B.; Tao, Y. T.; Evall, J.; Whitesides, G. M.; Nuzzo, R. G. *J. Am. Chem. Soc.* **1989**, *111*, 321−335.
(64) Ulman, A. *An Introduction to Ultrathin Organic Films; From Langmuir-Blodgett to Self-Assembly*; Academic Press: San Diego, 1991.
(65) Porter, M. D.; Bright, T. B.; Allara, D. L.; Chidsey, C. E. D. *J. Am. Chem. Soc.* **1987**, *109*, 3559.
(66) Miller, C.; Cuendet, P.; Gratzel, M. *J. Phys. Chem.* **1991**, *95*, 877.
(67) Becka, A. M.; Miller, C. J. *J. Phys. Chem.* **1993**, *97*, 6233−6239.
(68) Gennett, T.; Weaver, M. J. *Anal. Chem.* **1984**, *56*, 1444−1448.
(69) Hupp, J. T.; Weaver, M. J. *J. Phys. Chem.* **1985**, *89*, 2795−2804.
(70) Wipf, D. O.; Kristensen, E. W.; Deakin, M. R.; Wightman, R. M. *Anal. Chem.* **1988**, *60*, 306−310.

(71) Voltammetric scans to significantly more negative potentials resulted in slow deterioration of the films which begin to desorb at ca. −0.75 V.

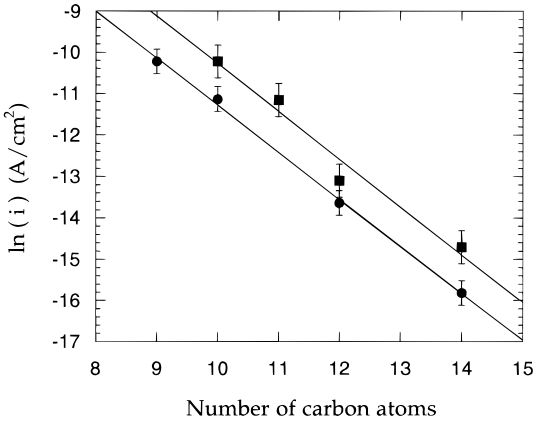

Figure 6. Plots of the logarithm of the tunneling current density vs number of the alkanethiolate chain carbon atoms recorded at −0.65 V at the HMDE coated with the ω-hydroxyalkanthiolate (square symbols) and alkanethiolate monolayers (closed circles) in a 1.0×10^{-3} M $Ru(NH_3)_6^{3+}$, 0.50 M KCl solution.

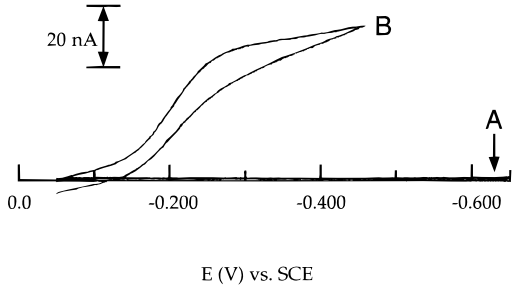

Figure 7. Cyclic voltammograms recorded in 1.0×10^{-3} M $Ru(NH_3)_6^{3+}$, 0.50 M KCl solution at a HMDE coated with an octadecanethiolate monolayer before and upon Hg drop expansion. The Hg drop surface areas are **A**, 0.02458, 0.02543, and 0.02628 cm^2 and **B**, 0.02710 cm^2; $v = 50$ mV/s.

Å to the film thickness. We can hypothesize that access of $Ru(NH_3)_6^{3+}$ to the hydrophobic methyl-terminated monolayers is restricted by the interfacial water to a larger extent than in the case of the hydrophilic hydroxyalkanethiols. A similar effect was observed recently by Becka and Miller in the case of ferricyanide reduction across methyl and hydroxy-terminated alkanethiol monolayers on gold electrodes.[67]

Properties of Mercuric Alkanethiolate Monolayers as Tunneling Barriers. B. Expanded Films. The use of a micrometrically driven HMDE and the ability to control the size of the Hg drop electrode opens a novel possibility to investigate the properties of the alkanethiolate films during Hg drop expansion. Our experimental data set is limited to the alkanethiols since their hydroxylated derivatives yielded thus far significantly less reproducible results. In these experiments, carried out in an aqueous KCl electrolyte following medium transfer from the hexadecane alkanethiol solution, the properties of the films depend strongly on the length of the alkyl chain. Consider two cases: (a) of alkanethiols with chain length above C_{14} represented by octadecanethiol in Figure 7 and (b) of alkanethiols with medium length chains, C_9-C_{14}, represented by dodecanethiol in Figure 8.

In the case of longer alkyl chain monolayers, only a small increase (5−7%) of the HMDE surface area is allowed before further increase of the HMDE surface area leads to creation of the defect sites through which $Ru(NH_3)_6^{3+}$ ions can be reduced at a mass transfer controlled rate. This results in sigmoidal, scan rate independent voltammograms as shown in Figure 7 indicating that at least one dimension of the defects is in a submicron to micron range.[72] At the current scale used to record

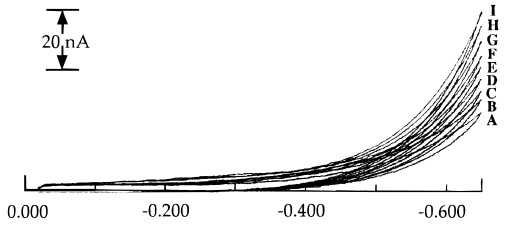

Figure 8. Cyclic voltammograms recorded in 1.0×10^{-3} M $Ru(NH_3)_6^{3+}$, 0.50 M KCl solution at a HMDE coated with an dodecanethiolate monolayer before and upon Hg drop expansion. The Hg drop surface areas are **A**, 0.024 58; **B**, 0.024 53; **C**, 0.026 28; **D**, 0.027 10; **E**, 0.027 92, **F**, 0.028 72; **G**, 0.029 52; **H**, 0.030 30; **I**, 0.031 08 cm^2; $v =$ 50 mV/s.

the voltammograms in Figure 7, the tunneling current recorded before the critical electrode expansion (three successive traces corresponding to a combined 6.9% increase of the initial surface area) is all but invisible in the plot (curve A). The magnitude of the plateau current (obtained after a combined 10.2% area increase) can be readily interpreted in terms of the surface area of the exposed clean mercury by modeling it as a single disk-shaped defect (with radius R) for which the current expression is well-known, $i = 4nFRDC$,[72] where D and C are the diffusion constant and concentration of $Ru(NH_3)_6^{3+}$. The exposed area of Hg (consisting likely of many pin-hole or line defects) generating the sigmoidal current in Figure 7 corresponds to 6.0% of the initial surface area of the drop. These observations lead us to picture the octadecanethiolate monolayers (and other monolayers with chain length above C_{14} which exhibit similar behavior) as essentially rigid thin films easy to fracture upon expansion in excess of ca. 5%. Monolayers with chain lengths shorter than C_9 revealed similar structural instability upon expansion. Such instability was also reported in the literature.[59] It is interesting to note that the recent grazing-incidence X-ray diffraction studies of alkanethiol monolayers on liquid mercury by Magnussen and co-workers failed to identify any in-plane order for any of the alkanethiols independent of their chain length (from C_8 to C_{30}).[73] Lack of long-range order expected for C_{18} (and longer alkanethiol) and known to exist in their monolayers on gold[31] was explained by the dominance of strong interactions of thiols with disordered mercury over weaker interactions within the hydrocarbon region.

Behavior of the intermediate chain length monolayers (C_9-C_{14}) is substantially different. These monolayers maintain their impermeable, barrier properties even upon sizable Hg drop expansion (up to ca. 30%). This can be deduced from the exponential character of the $Ru(NH_3)_6^{3+}$ reduction current which continues to be limited by slow electron tunneling kinetics at every stage of the drop expansion as shown in Figure 8 for the dodecanethiol case. Excessive expansions as well as excessively rapid expansions lead, however, to monolayer fracture that can be unambiguously recognized by a sharp current increase. These observations lead us to postulate that the monolayers with these chain lengths behave as continuous, liquid films.

This postulate can be verified by measuring changes of the interfacial capacitance of the thiolate-coated HMDE during drop expansion. The liquid monolayer model predicts that the product of the initial film thickness and the electrode surface area or the film volume (V_f) should stay constant. Thus the

(72) Howell, J. O.; Wightman, R. M. *Anal. Chem.* **1984**, *56*, 524−529.
(73) Magnussen, O. M.; Ocko, B. M.; Deutsch, M.; Regan, M. J.; Pershan, P. S.; Abernathy, D.; Gruebel, G.; Legrand, J.-F. *Nature* **1996**, *384*, 250−252.

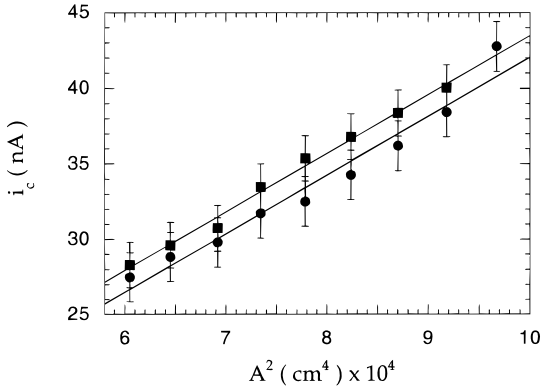

Figure 9. Plots of the charging currents recorded on HMDEs coated with decanethiolate (square sympols) and dodecanethiolate (closed circles) during Hg drop expansion. The initial surface area and the range of expansions are the same as those in Figure 8. The other experimental conditions are the same as in Figure 4.

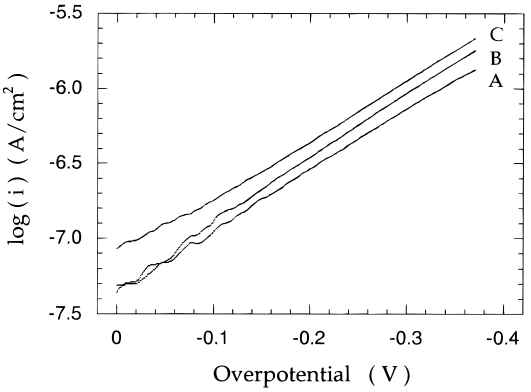

Figure 10. Tafel plots obtained from the current-voltage curves in Figure 8 after charging current background subtraction. Plots **A**, **B**, and **C** correspond to the traces **A**, **E**, and **I** in Figure 8.

interfacial capacitance (μF) given by

$$C = \epsilon\epsilon_o A/d \tag{1}$$

together with $Ad = V_f = \text{const}$ can be expressed by

$$C = \epsilon\epsilon_o A^2/V_f \tag{2}$$

Our measurements verified the linear dependence of the interfacial capacitance on the *square* of the electrode surface area as shown by the plot of charging current, $i_c = Cv$, in Figure 9 for the decane and dodecanethiolate monolayers. The slope of this dependence gave the dielectric constant of 2.0 ± 0.2 (average and standard deviation of 10 series of experiments for $C_{12}SH$) in agreement with our measurements of Figure 4. Thus the thickness of alkanethiol monolayers varies inversely proportionally with the electrode surface area, while the dielectric properties of the film remain unchanged.

In Figure 10, we plot the data from Figure 8A,E,I in the format of Tafel plots. Their linearity and invariance of the slope with the Hg drop expansion except in the region of low overpotentials provide an additional support of the continuous, defect-free characteristic of these alkanethiolate films. A small deviation from linearity at low overpotentials observed for some monolayers in their most expanded state (see Figure 10C) forecasts the limit of monolayer expansion. Such deviation could be interpreted as due to mass transport controlled current at a small number of pin-hole defects. The magnitude of this current is, however, negligible compared with the tunneling current at −0.65 V that is used in the analysis of the tunneling pathways (see next section).

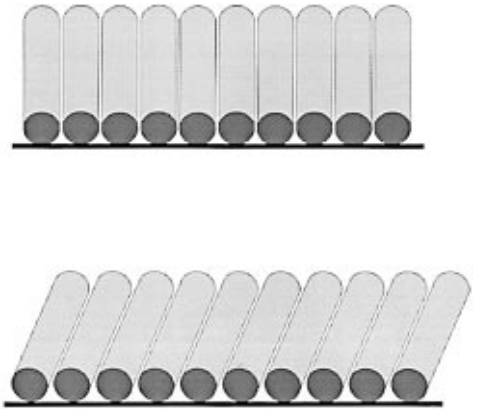

Figure 11. Schematic representation of the alkanethiolate monolayer expansion. The aspect ratio of the width and the length of the cylinders reflects approximately the dimensions of dodecanethiolate.

Thus, in molecular terms, we postulate that the decrease of the geometric film thickness in the expansion experiments involves a gradual tilting of the alkanethiol chains that maintains their volume, density, and dielectric properties. Depending on the actual fluidity of these films, their structure at a particular average tilt angle is expected to be at least to some extent dynamic and may involve several different conformations which nevertheless all have the same properties and can be represented by the simplest one with all-trans chain conformation and an average tilt as shown in Figure 11. The dynamic nature of the monolayer can be illustrated by the following: we observed routinely transitory break-up of dodecanethiolate monolayers when an individual expansion step of 2−3% was executed faster than over 2−3 s. However, defects created in those instances always disappeared within seconds, and the barrier character of a monolayer was fully restored, as long as the combined expansion of the monolayer at that point did not exceed its maximum limit of 25 −30%. In spite of these signs of a fluid nature of dodecanethiolate monolayers, it is likely that when viewed on a shorter time scale, these monolayers are structurally more ordered, perhaps even resembling those assembled on gold substrates. As mentioned above, the expansion experiments done with hydroxy-terminated monolayers have been much less successful. It is possible that the more ordered and stable structures of methyl-terminated monolayers is promoted by the dynamically ordered structure of water at the monolayer-solution interface.

Through-Bond vs Through-Space Coupling. Since these results allow us to calculate the geometric thickness of the film at every stage during the expansion experiments, we are, therefore, able to interpret the current increase in Figure 8 in terms of the apparent distance dependance of the electron tunneling rate. Figure 12 shows two plots of the logarithm of current measured at −0.65 V vs the geometric film thickness. The data set corresponding to the results of Figure 8 shows that the current increase upon film expansion is about 20 times smaller than one would expect for the 26% decrease of the geometric film thickness *assuming that the monolayer behaves as an isotropic dielectric barrier* in which electron tunneling efficiency is independent of its molecular structure. Clearly, therefore, this assumption does not hold. The large discrepancy between the observed and the expected current increase constitutes a strong evidence that electron tunneling proceeds primarily through the alkyl chains, a pathway which does not change in length in the course of the monolayer expansion. While this has been largely an undisputed postulate in most of

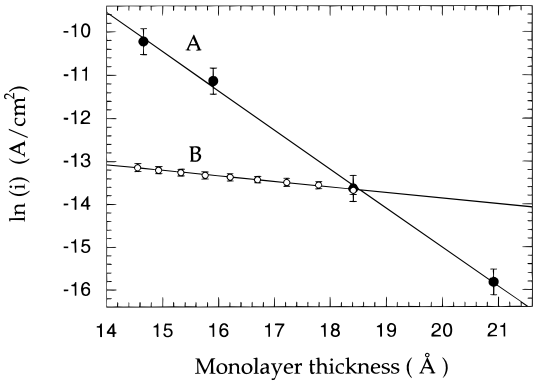

Figure 12. Plots of the logarithm of the tunneling current density vs the geometric film thickness. **A**, data recorded at the HMDE coated with alkanethiolate monolayers of different chain length (see Figure 6). **B**, data recorded at a HMDE coated with a dodecanethiolate monolayer during Hg drop expansion (as in Figure 8). Error bars are the two standard deviations of the average of four independent series of the expansion experiments.

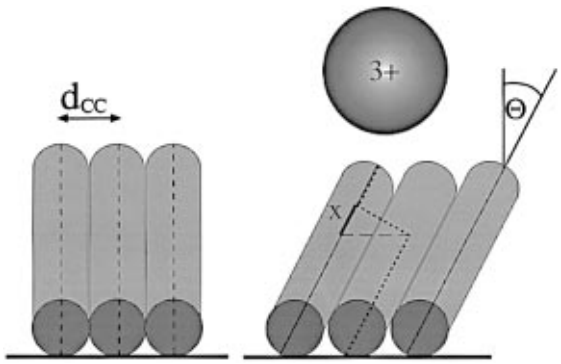

Figure 13. Schematic representation of the two electron tunneling pathways. In the perpendicularely oriented alkanethiolate monolayers, the through-bond pathway dominates. As the chains tilt, the additional pathway (marked by the densely dashed line) involves a chain-to-chain coupling. Segment marked **x** corresponds to the decrease of the through-bond pathway length realized upon chain-to-chain "hop". The dimensions of the cylinders and of the 3+ ion reflect approximately the dodecanethiolate monolayer and the size of hydrated $Ru(NH_3)_6^{3+}$.

the reports dealing with alkanethiol monolayers on gold electrodes, this is the first direct evidence that the through σ-bond path is, indeed, the dominant pathway in electron tunneling across these films. Nevertheless, the fact that a small current increase is observed in Figure 12B suggests that, in addition to the through σ-bonds, there exists another tunneling pathway along which the tunneling efficiency increases upon monolayer expansion.

We postulate that this new tunneling pathway involves intermolecular coupling between adjacent hydrocarbon chains. As the average tilt angle of the monolayer increases upon expansion of the Hg droplet, electronic coupling pathways involving lateral hops between hydrocarbon chains become more important in the overall electron tunneling rate. This point can be illustrated graphically by considering the decrease of the electron tunneling distance in a pathway involving a lateral hop between the adjacent alkyl chains. Both pathways are marked in Figure 13. Our model assumes that the total coupling involves a sum of through-bond and through-space interactions between adjacent methylene groups within the monolayer assembly. Thus, individual pathways may involve either solely through-bond interactions, or they may combine these with one or more through-space hops (chain-to-chain coupling). It is apparent in this parallel pathways model that the length of pathways involving through-space hops (marked with a densely dotted line in Figure 13) decreases with the tilt of the alkanethiol chains by $x = d_{cc}\mathrm{tg}\Theta$ for each lateral hop. For example, the tunneling distance along the pathway involving one lateral hop shown schematically in Figure 13 is $d - d_{cc}\mathrm{tg}\Theta + d_{cc}$. Pathways which contain only through-bond interactions are anticipated to be most important in determining the rate of electron tunneling through the alkanethiol monolayer film. Since coupling across the van der Waals bridge between two adjacent chains is expected to be relatively inefficient, pathways that include a single lateral hop are next in significance. If one neglects pathways that contain more than one lateral hop, a relatively simple expression for the observed current as a function of the monolayer tilt angle can be derived:

$$i_t = i_o \exp(-\beta_{tb} d) + i_o n_s \exp[-\beta_{tb}(d - d_{cc}\mathrm{tg}\Theta)] \times \exp(-\beta_{ts} d_{cc}) \quad (3)$$

Here i_t is the observed current density measured at a particular average monolayer tilt, Θ, i_o is the current density anticipated in the absence of the monolayer film, n_s is a statistical factor accounting for increased number of pathways containing a single lateral hop as compared to those containing only through-bond hops, d is the length of the tunneling pathway along the alkane thiol chains (for dodecanethiolate $d = 18.41$ Å),[74,75] $d_{cc} = 4.75$ Å is the contact distance between adjacent alkyl chains modeled as cylinders, and β_{tb} and β_{ts} are, respectively, through-bond and through-space decay constants. In order to use this equation to obtain estimates of β_{tb} and β_{ts}, one must obtain an estimate of the i_o and n_s. The current density in the absence of the monolayer film can be determined from an extrapolation of the logarithm of the current density versus monolayer thickness obtained for a series of monolayers composed of alkanethiols of different length at zero tilt (see Figure 6). The i_o value obtained by assuming that only the pure through-bond pathway contributes significantly to the observed current density at zero monolayer tilt is 24.8 A/cm^2. The statistical factor, n_s, can be estimated to a first approximation as the number of carbon atoms in the alkanethiol chain used to form the monolayer. This is 12 in the case of dodecanethiol for which the most extensive data set was collected and analyzed below.[76]

A least square fit of eq 3 to the average of four independent sets of current density (weighted by their standard deviations) versus monolayer tilt data (see Figure 14) yields the values of both β_{tb} and β_{ts} as the fitting parameters. The β_{tb} was determined to be 0.91 ± 0.01 Å^{-1}, while the β_{ts} was found to be 1.31 ± 0.05 Å^{-1} ($\chi^2 = 1.58$, $R^2 = 0.96$). Considering the uncertainties in the values of i_o, d, and n_s, the true uncertainties in the fitting parameters are likely larger. We note the relatively large deviation of the current at $\Theta = 0$ from the fitted curve. This is perhaps due to the fact that, initially, the monolayer could be locked in a nonequilibrium structure containing, for example, excessive number of gauche defects or 2D solid domains of different than equilibrium sizes that result in lower tunneling rates either because of lower electronic coupling or due to different interfacial water structure that affects access of

(74) The thickness of the all-trans, perpendicularly oriented mercuric alkanethiolate monolayer with n carbon atoms was calculated as a sum of the following surface normal projected bond lengths (see ref 75): 0.5 × Hg-S (1.1 Å) + CH_2-S (1.5 Å) + (n−1) × CH_2-CH_2 (1.255 Å) + vdW radius of the terminal methyl group (2.0 Å).

(75) Fraser, K. A.; Clegg, W.; Craig, D. C.; Scudder, M. L.; Dance, I. G. *Acta Crystallogr. C* **1995**, *51*, 406−408.

(76) The value of $n_s = 12$ is correct for the 2D, cross-sectional model of the dodecane monolayer presented in Figure 13. Its value should be somewhat larger when a real 3D structure of the film is taken into account. Since increasing n_s by as much as 50% leads only to a 6% increase of β_{ts} in the fit shown in Figure 14, for the sake of clarity, we use $n_s = 12$ as an adequate approximation.

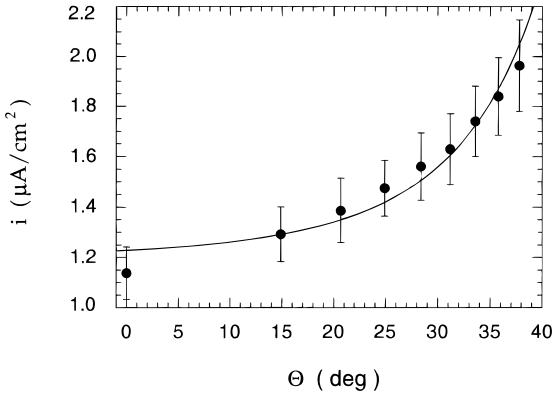

Figure 14. Plot of the tunneling current density measured at −0.65 V during electrode expansion as a function of the average tilt angle of the dodecanethiolate chains (see Figure 11). Data points are the average values of the current obtained in four independent series of experiments featured in Figure 8. The line is a least squares fit (using Levenberg−Marqurdt algorithm) of eq 3 to the data.

the redox probe. We observed frequently a small current histeresis upon Hg drop recompression to its initial volume, resulting in a larger value of the tunneling current at $\Theta = 0$. Short of this discrepancy, we judge the fit in Figure 14 to be very good and to support the validity of the model. Moreover, the value of β_{tb} obtained as a fitting parameter is identical to that obtained in the classical way featured in Figures 6 and 12. As expected, the strength of the chain-to-chain coupling is significantly weaker. In relative terms, the rate decay encountered in tunneling across a d_{cc} space between two alkyl chains is equivalent to the rate loss in tunneling across 5.5 σ-bonds. Our value of the coupling strength across a van der Waals bridge is larger than the estimate of Gray and co-workers who deduced that the rate loss in tunneling across a van der Waals bridge in cytochrome *c* (of 3.88 Å) is equivalent to the rate decay encountered in tunneling across 10.6 σ bonds.[77] We judge our value of β_{ts} to be more reliable because it stems from more direct measurements involving a substantially simpler system.

***Ab Initio* Estimates of Through-Space and Through-Bond Coupling.** The electronic coupling through molecular assemblages can be modeled via *ab initio* methods. In particular, the rate of tunneling through a molecular spacer can be estimated in a variety of ways. In the past we have successfully employed a Koopmans' theorem approximation for the electronic coupling matrix element to predict the affect of small structural changes to hydrocarbon spacers on the rate of electron transfer across such hydrocarbons.[43] The predicted tunneling rates were in good agreement with experiment. These calculations were also extended to probe possible quantum interference effects within hydrocarbon monolayers.[44]

In the KT method, the splitting between symmetric and antisymmetric combinations of radical reporter groups separated by a rigid molecular spacer are calculated via an unrestricted Hartree−Fock, SCF approach.[40,41,78−80] We have focused on the splitting between symmetry equivalent nonbonded Li atoms. In the Fermi's golden rule limit appropriate for weakly electronically coupled systems, the probability of electron tunneling from one radical to the other is proportional to the square of the Li splitting energy. In order to obtain an estimate

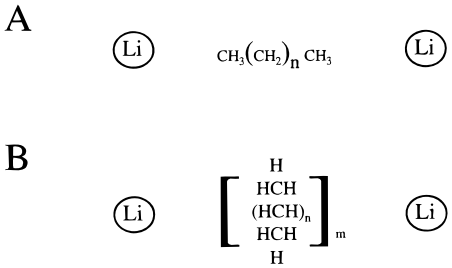

Figure 15. Schematic representation of the position of the Li reporter atoms and n-alkanes used in the computations of the distance dependence of the electronic coupling matrix elements of the through-bond (**A**) and through-space (**B**) electron tunneling.

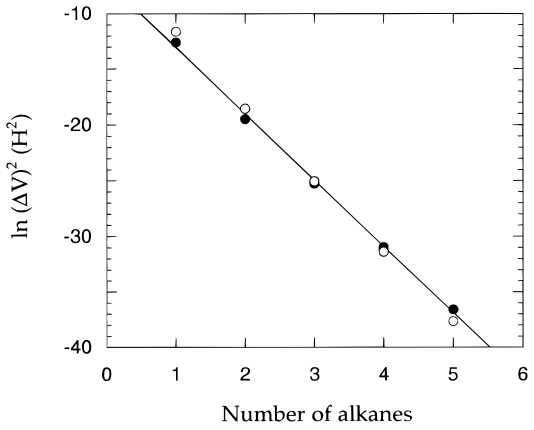

Figure 16. Plots of the logarithm of squares of the splitting energy of neutral Li−Li triplet across a number of alkanes oriented as shown in Figure 15B. Open circles correspond to the methane and closed circles to the heptane data set.

of the through-bond and through-space electron tunneling decay constants, β_{tb} and β_{ts}, a series of calculations were performed on pairs of Li atoms separated by hydrocarbons of various lengths and orientations as shown in Figure 15. For a pair of Li radicals positioned 4 Å from the terminal methyl groups of n-alkanes, a plot of $\ln(\Delta V)^2$ versus the number of methylene groups within the hydrocarbon spacer yields a β_{tb} estimate of 1.097 per methylene group or 0.88 Å^{-1}. This is in very good agreement with our measurements reported above and other experimentally[31,34−39] and theoretically determined values.[40−42]

An estimate of the through-space tunneling coefficient, β_{ts}, was obtained using hydrocarbon spacers oriented normal to the Li−Li direction (Figure 15B). The distance between the two Li radical reporters was increased by increasing the number of the parallel hydrocarbon chains composing the spacer. We find that Li atoms can be separated by 1−5 hydrocarbon chains before the Li splitting energy becomes too small to be measured. As the n-alkanes are varied from methane to heptane, the tunneling coefficient obtained from the $\ln(\Delta V)^2$ versus the number of hydrocarbon chains plot decrease from 1.37 to 1.25 Å^{-1} as shown in Figure 16. These estimates of the lateral tunneling decay coefficient, β_{ts}, are in remarkable agreement with that determined from the parallel pathways model.

This close agreement between the experiment and theory occurs in spite of several simplifications used both in the *ab initio* method and the formulation of the parallel pathways model. The geometry of the spacers used in the calculation is of necessity different than that present within the alkanethiol films on the Hg surface. For the β_{ts} estimate, the relative orientation of the methylene groups with respect to the adjacent hydrocarbon chains are fixed in order to maintain the two Li radicals in symmetry equivalent positions. Instead of a nearly

(77) Wuttke, D. S.; Bjerrum, M. J.; Winkler, J. R.; Gray, H. B. *Science* **1992**, *256*, 1007−1009.
(78) Naleway, C. A.; Curtiss, L. A.; Miller, J. R. *J. Phys. Chem.* **1991**, *95*, 8434−8437.
(79) Liang, C.; Newton, M. D. *J. Phys. Chem.* **1992**, *96*, 2855−2866.
(80) Jordan, K. D.; Paddon-Row, M. N. *J. Phys. Chem.* **1992**, *96*, 1188−1196.

hexagonal array of hydrocarbon chains present in the monolayer, a single row of hydrocarbon chains is used in the calculation. Similarly, in the β_{tb} estimate, only a single hydrocarbon was used.

The parallel pathways model assumes that the through-bond electronic coupling is independent of the tilt angle (see eq 3). In reality, it is likely that the decrease in the surface density of the hydrocarbon chains upon Hg electrode expansion would result in a concomitant decrease in the through chain component of the electron transfer rate. Appearance of the gauche defects in the alkane chains as the tilt angle increases would likewise result in the decrease of the through-bond coupling efficiency.[6,81,82] Consideration of these factors suggests that our β_{ts} is perhaps an upper bound estimate of the true value. The initial perpendicular orientation of the dodecanethiolate chains ($\Theta = 0$) was adopted as a simplifying approximation in spite of a small deviation of the experimentally determined packing density from the calculated value (20.3 vs 19.5 Å^2/molecule). Taking this into account would yield an initial tilt angle, $\Theta_{initial} = 16.1°$ and increase the final value of the monolayer tilt from 37.8° to 40.8°. However, these modifications introduce only negligible changes in the quality of the fit and in the values of the fitting parameters (β_{tb} increases from 0.91 to 0.92 and β_{ts} from 1.31 to 1.37).

Finally, we consider our model describing an alkanethiolate monolayer as a constant volume viscous liquid to be a simplification itself. While the presented data support the model adequately, more experimental investigations need to be carried out to test it further. Specifically, the extent to which dodecanethiolate and similar monolayers on mercury can be regarded as liquid films need to be studied further. Thus, for example, investigations involving more hydrophobic redox probes and temperature studies will be useful to provide a more insightful picture of this system and its behavior in the Hg drop expansion experiments.

Conclusions and Summary of Results

Formation of alkanethiol monolayers on mercury, while similar in many aspects to the process on gold, brings about several advantages relating to their preparation, procedure, and structure. The most important advantages stem, however, from the use a micrometrically driven HMDE. Specifically, we showed that constant potential coulometry combined with Hg drop extrusion offers a direct method for the coverage determination that is essentially free of the uncertainties due to double-layer charge usually encountered in the potential step and voltammetric methods. Secondly, our earlier observation that a Hg drop covered with an alkanethiol monolayer can be enlarged to increase its surface area by as much as 30% without generating pin-hole defects opened a possibility to analyze the observed tunneling current in terms of two different pathways involving through-bond and chain-to-chain coupling. These experiments and their analysis gave the first direct assessment of the decay constant characterizing the coupling strength across a van der Waals bridge, $\beta_{ts} = 1.31 \pm 0.05$ Å^{-1}. This value is in excellent agreement with an estimate obtained by *ab initio* calculations. The following is a more detailed summary of the key results.

Chemisorption of alkanethiols on mercury proceeds on a millisecond time scale and involves a two-electron oxidation of mercury to form of mercuric thiolate ($Hg(SR)_2$) in a broad range of potentials (−0.5 to 0.3 V vs SCE for a dodecanethiol). Application of a micrometrically driven hanging mercury drop electrode enabled us to carry out coulometric coverage measurements involving constant potential Hg drop extrusion. These experiments showed that alkanethiolates with the chain length above C_8 form passivating monolayers with closely packed chains oriented perpendicular to the electrode surface. The barrier properties of these monolayer films were characterized by differential capacitance measurements and via electron tunneling experiments. The latter yielded the through-bond decay constant $\beta_{tb} = 1.14$ per CH_2 when alkanethiols from nonane to tetradecane were used to vary the thickness of the monolayer. This result is very similar to the measurements of the decay constant with alkanethiol monolayers on gold electrodes.

Slow expansion of Hg drop covered with an alkanethiolate monolayer (with chain length in the range C_9−C_{14}) in an aqueous electrolyte containing $Ru(NH_3)_6^{3+}$ ions does not result in generation of defects but rather produces a 70% increase in the tunneling current. These monolayers maintain their impermeable character even upon 25−30% increase of the Hg drop surface area. To understand this behavior, we first showed that these monolayers behave like constant volume liquid films, and thus their thickness decreases inversely proportionally to their surface area. The body of experimental data involving the capacitance, coulometric, and tunneling measurements led us to postulate that the structure of the monolayers can be approximated by a model involving all-trans alkane chains tilting from their initial perpendicular orientation in response to drop expansion to decrease their geometric thickness, while maintaining their constant volume and dielectric properties.

In view of this model, the analysis of the tunneling current during drop expansion showed conclusively that through σ-bonds of the alkane chains is the predominant pathway of electron tunneling. To account for an increase of the tunneling current density in these experiments, we constructed a parallel pathways model which identifies a possibility of electronic coupling between the alkane chains. A least square fit of the ensuing equation to the data gave the values of both through-bond and through-space decay constants. The former, $\beta_{tb} = 0.91$ Å^{-1}, is identical to the value obtained on the basis of the tunneling experiments involving monolayers formed by alkanethiols of different chain length. The latter, $\beta_{ts} = 1.31$ Å^{-1}, is the first direct measurement of the decay constant involving noncovalently bonded molecular segments. This value agrees well with β_{ts} obtained via *ab initio* calculations for a geometrically simple planar array of n-alkanes involving Koopmans' theorem approximation in the calculations of the electronic coupling matrix element. As expected, the magnitude of β_{ts} reflects weaker through-space coupling compared to one for a σ-bonded alkane chains. Its value is similar to an earlier estimate of the coupling efficiency across a van der Waals bridge in proteins.

Acknowledgment. The authors gratefully acknowledge financial support of the U.S. National Science Foundation under Grants CHE-9422619 and CHE-9417357. Partial support was also provided by a Polish KBN Grant 3T09A09908. M.M. expresses gratitude to Professor Dr. Dietmar Möbius for his hospitality at M-P-I für biophysikalische Chemie in Göttingen during the 1996/97 sabbatical.

JA971921L

(81) Jordan, K. D.; Paddon-Row, M. N. *Chem. Rev.* **1992**, *92*, 395−410.

(82) Haran, A.; Waldeck, D. H.; Naaman, R.; Moons, E.; Cahen, D. *Science* **1994**, *263*, 948−950.